Inorganic Chemistry

Article

pubs.acs.org/IC

Alkali Metal Variation and Twisting of the FeNNFe Core in Bridging Diiron Dinitrogen Complexes

Sean F. McWilliams,[†] Kenton R. Rodgers,[‡] Gudrun Lukat-Rodgers,[‡] Brandon Q. Mercado,[†] Katarzyna Grubel,[†,§] and Patrick L. Holland*[,†]

[†]Department of Chemistry, Yale University, 225 Prospect Street, New Haven, Connecticut 06520, United States

[‡]Department of Chemistry and Biochemistry, North Dakota State University, Fargo, North Dakota 58105, United States

Supporting Information

ABSTRACT: Alkali metal cations can interact with Fe−N_2 complexes, potentially enhancing back-bonding or influencing the geometry of the iron atom. These influences are relevant to large-scale N_2 reduction by iron, such as in the FeMoco of nitrogenase and the alkali-promoted Haber−Bosch process. However, to our knowledge there have been no systematic studies of a large range of alkali metals regarding their influence on transition metal−dinitrogen complexes. In this work, we varied the alkali metal in [alkali cation]$_2$[LFeNNFeL] complexes (L = bulky β-diketiminate ligand) through the size range from Na^+ to K^+, Rb^+, and Cs^+. The FeNNFe cores have similar Fe−N and N−N distances and N−N stretching frequencies despite the drastic change in alkali metal cation size. The two diketiminates twist relative to one another, with larger dihedral angles accommodating the larger cations. In order to explain why the twisting has so little influence on the core, we performed density functional theory calculations on a simplified LFeNNFeL model, which show that the two metals surprisingly do not compete for back-bonding to the same π^* orbital of N_2, even when the ligand planes are parallel. This diiron system can tolerate distortion of the ligand planes through compensating orbital energy changes, and thus, a range of ligand orientations can give very similar energies.

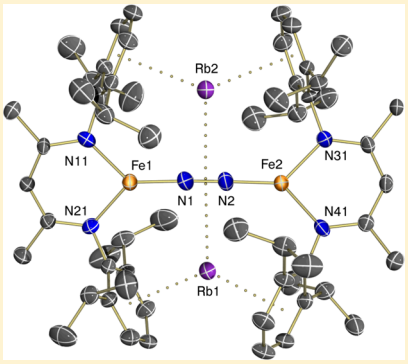

INTRODUCTION

Nitrogen is an essential element for life. However, its most abundant form, N_2, contains a strong N−N triple bond (226 kcal/mol) that must be cleaved to provide biologically available nitrogen compounds such as ammonia.[1] Nitrogen fixation, the process of converting dinitrogen to ammonia, occurs mainly in two ways: a natural process in nitrogenase enzymes at a predominantly iron cofactor and a high-temperature, high-pressure process (Haber−Bosch) that most commonly uses a reduced heterogeneous iron catalyst with aluminum and potassium dopants.[2−4] Atomic resolution of the mechanism for N−N bond cleavage and subsequent ammonia formation remains elusive for each process.[5]

Studies on iron surfaces have led to an understanding of the microstructure of the iron catalyst for the Haber−Bosch process.[3] Experiments on single crystals of Fe with known crystal facets have shown that the Fe(111) surface is the most active for catalysis under high-pressure conditions.[6] Experiments on these idealized Fe surfaces show that small concentrations of potassium on the surface decrease the work function of the solid (i.e., raise the energy of the highest-lying electrons), implying that electron donation from the surface to bound dinitrogen species would be easier.[7] In molecular terms, this corresponds to stronger back-bonding from higher-energy Fe d orbitals into N_2, resulting in a weakened N−N bond. Adsorption of potassium on these promoted iron surfaces enhances the binding of N_2 to the surface.[8] However, molecular examples of iron−potassium−N_2 complexes, which would test this idea and explore it in atomic detail, are rare.[9,12,13]

Hundreds of examples of transition metal−N_2 complexes have been reported in the literature, and they are known with most transition metals.[1,10] Only a small percentage of these also contain an interaction between the bound N_2 moiety and an alkali cation, limiting our understanding of how these positively charged ions effect N−N bond activation.[11−13] Most of the complexes with interactions between the alkali cation and N_2 have an end-on (η^1) interaction.[11] In several examples, the end-on coordination by the alkali cation is disrupted by sequestration of the cation by multiple crown ethers (Figure 1) or by cation exchange to a noncoordinating ion, which increases the energy of the N−N stretching vibration by 20−40 cm^{-1}.[11] This difference in stretching frequency implies that positively charged redox-inactive alkali cations activate the N_2 unit when bound in an end-on fashion.

Less common are coordination compounds with a side-on (η^2) interaction between alkali cation(s) and a transition-metal-bound N_2 unit.[12−14] These may be relevant to the cleavage of N_2 on iron surfaces because the precursor to N−N cleavage on the surface has been shown to have the N−N bond roughly parallel to the surface,[15] and in this geometry side-on interactions of surface atoms with N_2 are likely. In many of

Received: December 10, 2015
Published: March 1, 2016

DOI: 10.1021/acs.inorgchem.5b02841
Inorg. Chem. 2016, 55, 2960−2968

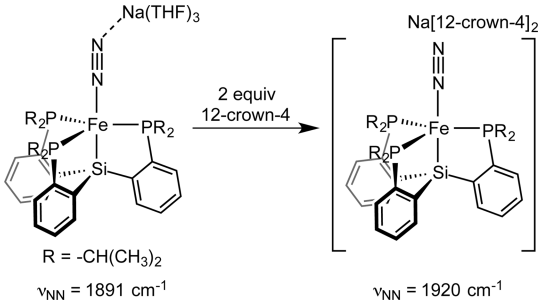

Figure 1. An example of the effect of sequestration of a terminally bound alkali metal cation on the N−N stretching frequency.[11f]

the molecular compounds with side-on alkali interactions, the alkali cations are labile, which impedes the study of the influence of coordination of these cations on N−N bond activation.[14]

β-Diketiminate-supported bridging N_2 complexes are particularly amenable to such investigations because they have been studied systematically.[16] In the Fe, Co, and Ni systems, binding of N_2 occurs upon reduction of M^{II} halide precursors to the M^{I} oxidation state, yielding end-on/end-on bridging dinitrogen complexes (Figure 2a).[12,13] Further reduction by two electrons

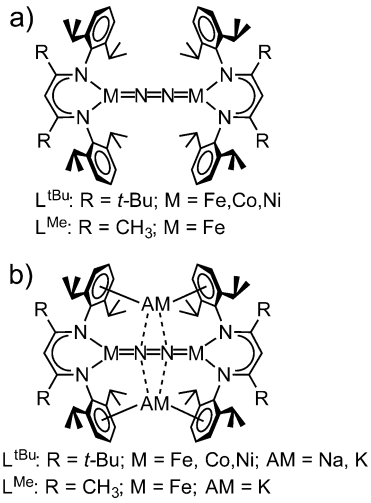

Figure 2. (a) Formally M^{I} β-diketiminate-supported dinitrogen complexes. (b) Formally M^{0} β-diketiminate-supported dinitrogen complexes with alkali metal (AM) cations side-on to the N_2 unit.[12,13]

yields formally M^{0} complexes with sodium or potassium bound side-on to the N_2 and to the aryl rings of the β-diketiminate ligands (Figure 2b).[12,13] The alkali metal cations in these complexes are not coordinated by solvent in the solid-state structures, and there is no evidence for cation lability in noncoordinating or weakly coordinating solvents. The lack of lability of these cations and their close proximity to the N_2 unit make these systems ideal for studying the influence of alkali metal cations bound side-on to dinitrogen in iron complexes.

Complexes having each of these three transition metals in both the +0 and +1 oxidation states have been isolated and exhibit weakening of the N−N bond compared with free dinitrogen, as observed by crystallography and vibrational spectroscopy.[12,13] In each case, the formally M^{0} complex contains a substantially more activated N_2 unit (200−500 cm^{-1} lower stretching frequency) than the formally M^{I} complex.[12b,d]

For all three transition metals (Fe, Co, Ni), both sodium and potassium analogues have been synthesized using the larger β-diketiminate ligand L^{tBu}.[17] In the Co system, the Na^+ and K^+ analogues had similar N−N bonds, differing by less than 0.01 Å in the observed N_2 bond length and only 1 cm^{-1} in the observed N−N stretching frequency.[12b] In contrast, varying the alkali metal from Na^+ to K^+ in the Fe and Ni systems caused increases in the observed N−N stretching frequency by 6 and 14 cm^{-1}, respectively.[12a,c,d,13] A mixed-alkali species with both Na^+ and K^+ was isolated in the Ni system and exhibited an N−N stretching frequency that lies between those of the K^+ and Na^+ analogues.[12d] However, in each of these systems there were only two data points: Na^+ and K^+. Studies of the Haber−Bosch process have shown that the promotion effect increases in the order Na < K < Rb < Cs,[2,18] which indicates that the heavier alkali metals could be beneficial.

Here, for the first time, we explore the alkali metal trend in a series of analogous M−N_2 complexes with each alkali metal from Na^+ to Cs^+. We show that there is an interesting interplay between the size of the alkali metal ion and the dihedral angle between the diketiminate ligands on the two metals of the FeNNFe core. We evaluate the effects of twisting the core on the frontier orbitals of the FeNNFe core using density functional theory (DFT) calculations. Interestingly, despite the drastic change in the cation size and the twisting of the core, the extent of N−N bond weakening is very similar throughout the series.

RESULTS AND DISCUSSION

Synthesis and Characterization. In order to better understand the role of the cations in FeNNFe complexes, a series of compounds were synthesized from iron(II) halide complexes of L^{Me} using the alkali metal reductants Na, KC_8, RbC_8, and CsC_8 (Scheme 1). Synthesis of the K^+ analogue

Scheme 1. Synthesis of 2-AM (AM = Na, K, Rb, Cs)[a]

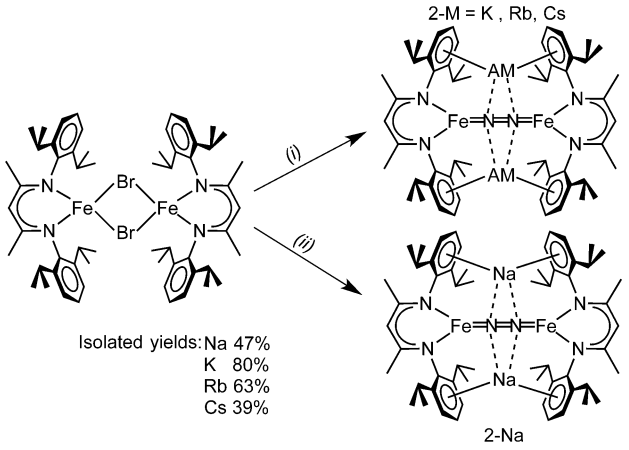

[a]Reaction conditions: (i) $4AMC_8$ (AM = K, Rb, Cs), pentane or diethyl ether; (ii) excess Na^0, diethyl ether.

$K_2[L^{Me}FeNNFeL^{Me}]$ (**2-K**) was previously reported through reduction of $[L^{Me}Fe(\mu\text{-}Cl)]_2$ with 4 equiv of potassium/graphite (KC_8) in pentane under N_2.[13] Here we synthesized **2-K** from $[L^{Me}Fe(\mu\text{-}Br)]_2$ (**1**) instead by a procedure adapted from those previously reported methods.[13,19] Reduction of $[L^{Me}Fe(\mu\text{-}Br)]_2$ with 4 equiv of rubidium/graphite (RbC_8) in pentane under N_2 and cesium/graphite (CsC_8) in diethyl ether under N_2 led to the formation of the dark-green complexes

DOI: 10.1021/acs.inorgchem.5b02841
Inorg. Chem. 2016, 55, 2960−2968

$Rb_2[L^{Me}FeNNFeL^{Me}]$ (**2-Rb**) and $Cs_2[L^{Me}FeNNFeL^{Me}]$ (**2-Cs**), respectively. Stirring $[L^{Me}Fe(\mu\text{-Br})]_2$ in diethyl ether with excess sodium metal yielded the dark-green complex $Na_2[L^{Me}FeNNFeL^{Me}]$ (**2-Na**). Samples of **2-Rb** and **2-Na** gave satisfactory microanalytical results, while **2-Cs** was consistently low in N; however, the ^{1}H NMR spectra were all comprehensible using averaged D_{2h} or D_{2d} symmetry. Solid-state molecular structures were obtained from crystals of each compound that were grown from diethyl ether or pentane, and thermal ellipsoid plots are shown in Figures 3 and 4. Sonication

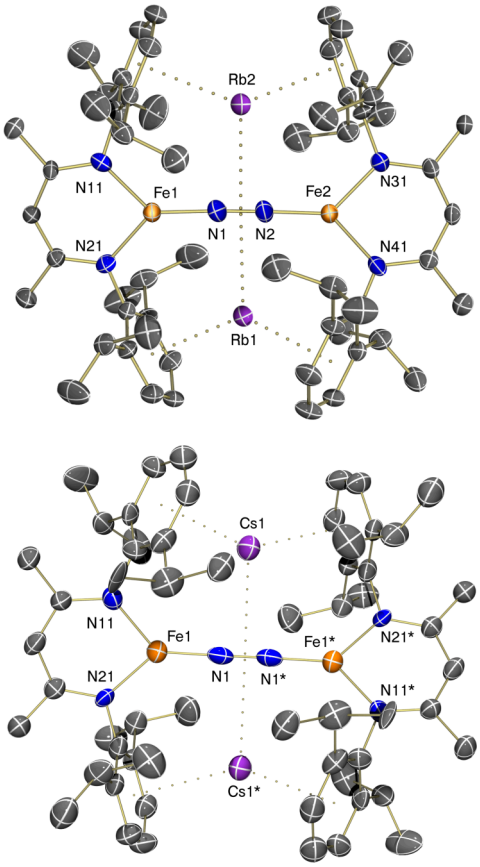

Figure 3. Molecular structures of (top) **2-Rb** and (bottom) **2-Cs**. Thermal ellipsoids are displayed at the 50% probability level. Hydrogen atoms have been omitted for clarity. Selected bond lengths (Å) and angles (deg) for **2-Rb**: Fe(1)−N(1) 1.740(7), Fe(1)−N(11) 1.928(6), Fe(1)−N(21) 1.938(6), Fe(2)−N(2) 1.741(7), Fe(2)−N(31) 1.933(6), Fe(2)−N(41) 1.931(6), N(1)−N(2) 1.257(8), Rb(1)−N(1) 2.908(7), Rb(1)−N(2) 2.869(6), Rb(2)−N(1) 2.918(7), Rb(2)−N(2) 2.931(7), N(11)−Fe(1)−N(21) 96.0(2), N(1)−Fe(1)−N(11) 131.8(3), N(1)−Fe(1)−N(21) 133.2(3), N(31)−Fe(2)−N(41) 95.0(2), N(2)−Fe(2)−N(31) 131.6(3), N(2)−Fe(2)−N(41) 133.2(3). For **2-Cs**: Fe(1)−N(1) 1.713(12), Fe(1)−N(11) 1.933(11), Fe(1)−N(21) 1.930(10), N(1)−N(1)* 1.33(2), Cs(1)−N(1) 3.087(10), Cs(1)−N(1)* 3.093(11), N(11)−Fe(1)−N(21) 95.6(4), N(1)−Fe(1)−N(11) 131.1(5), N(1)−Fe(1)−N(21) 133.2(4).

or stirring of $[L^{Me}Fe(\mu\text{-Br})]_2$ or $[L^{Me}FeNNFeL^{Me}]$ with excess Li^0 under N_2 yielded unidentifiable mixtures of compounds, none of which are spectroscopically analogous to the other **2-AM** compounds.

The N−N distances in all of these complexes show significant weakening of the bound dinitrogen, as previously demonstrated in **2-K**.[13] The N−N bond lengths in the solid-

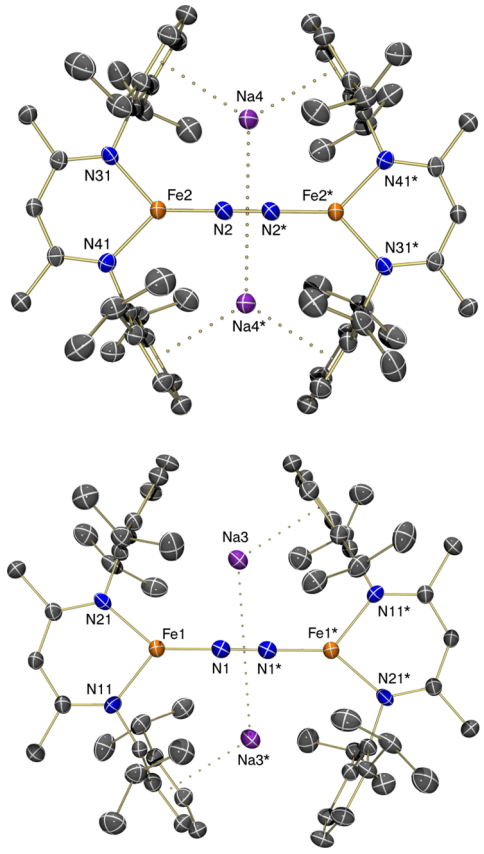

Figure 4. Molecular structure of **2-Na**. Two different conformations are present in the asymmetric unit: one with the sodium cations centered between the aryl rings of the supporting ligands (**2-Na (centered)**, top) and one with the sodium cations off-center between the aryl rings of the supporting ligand (**2-Na (not centered)**, bottom). Thermal ellipsoids are displayed at the 50% probability level. Hydrogen atoms have been omitted for clarity. Selected bond lengths (Å) and angles (deg) for **2-Na (centered)**: Fe(2)−N(2) 1.725(3), Fe(2)−N(31) 1.918(3), Fe(2)−N(41) 1.923(3), N(2)−N(2)* 1.253(6), Na(4)−N(2) 2.524(3), Na(4)−N(2)* 2.512(3), N(31)−Fe(2)−N(41) 94.76(11), N(2)−Fe(2)−N(31) 131.74(13), N(2)−Fe(2)−N(41) 133.41(13). For **2-Na (not centered)**: Fe(1)−N(1) 1.728(3), Fe(1)−N(11) 1.936(3), Fe(1)−N(21) 1.936(3), N(1)−N(1)* 1.254(6), Na(3)−N(1) 2.566(3), Na(3)−N(1)* 2.454(3), N(11)−Fe(1)−N(21) 93.15(11), N(1)−Fe(1)−N(11) 127.48(13), N(1)−Fe(1)−N(21) 139.14(13).

state molecular structures range from 1.215(6) to 1.33(2) Å and are substantially longer than that of free N_2 (1.098 Å) (Table 1).[20] The N−N bond lengths from the crystal structures are similar, except that the N−N bond in **2-Cs** is about 0.1 Å longer than that in **2-K**. Unfortunately, the precision (and probably the accuracy; see below) of the N−N bond length in **2-Cs** is poor because of either libration in the core or unavoidable Fourier truncation as a result of the large Cs atoms. In order to gain a more reliable view of the N−N bond weakening, we used resonance Raman spectroscopy with 406.7 nm laser excitation, as reported previously for **2-K**.[13] All four compounds showed vibrations between 1612 and 1625 cm^{-1} that shifted to lower frequency in $^{15}N_2$-enriched samples (Table 1). The low frequencies indicate significant N−N bond weakening relative to N_2 (2359 cm^{-1}) (Table 1).[21] The bond lengths and stretching frequencies are similar to those in diazene, HN═NH (1.25 Å and 1583 cm^{-1}, respectively), suggesting that each complex has a N−N double bond.[21a] **2-Cs**

DOI: 10.1021/acs.inorgchem.5b02841
Inorg. Chem. 2016, 55, 2960−2968

Table 1. Fe−N and N−N Bond Lengths, N−N Bond Stretching Frequencies, and Mössbauer Parameters for Bridging Fe−N_2 Complexes with Intercalated Alkali Cations

compound	Fe−N (Å)	N−N (Å)	ν_{NN} (cm^{-1})[b]	$\nu^{15}N^{15}N$ (cm^{-1})[c]	δ (mm/s)	$\lvert\Delta E_Q\rvert$ (mm/s)	ref
2-Na	1.728(3), 1.725(3)	1.254(6), 1.253(6)	1612	1559 [1557]	0.44	2.52	this work
2-K	1.750(4), 1.755(5)	1.215(6)	1625	1569 [1570]	0.47	2.48	13
2-Rb	1.740(7), 1741(7)	1.257(6)	1621	1567 [1566]	0.46	2.34	this work
2-Cs	1.711(12)[a]	1.33(2)[a]	1613	1566 [1558]	0.48	2.20	this work

[a]These values are likely influenced by a systematic error (see the text). [b]Experimentally observed $^{14}N^{14}N$ frequencies. [c]Experimentally observed $^{15}N^{15}N$ frequencies; the values in brackets are the $^{15}N^{15}N$ stretching frequencies expected on the basis of the harmonic oscillator approximation.

does not have a lower frequency than the others, indicating that the long N−N distance in the crystal structure is unlikely to be accurate.

Each complex exhibits one quadrupole doublet in the Mössbauer spectrum, indicating that the two iron centers have equivalent (or nearly equivalent) environments. The isomer shifts (δ) are 0.44−0.48 mm/s, and the quadrupole splitting values ($\lvert\Delta E_Q\rvert$) are 2.20−2.52 mm/s.

In the solid-state structures of these complexes, the backbones of the β-diketiminate supporting ligands rotate with respect to one another as the size of the intercalated cation increases (Figure 5). The aryl groups also rotate to create a larger distance between the centroids of the aryl rings, with an increase of 1.1 Å from **2-Na** to **2-Cs** (Table 2). The larger size of the alkali binding pocket is consistent with the larger ionic radii of the alkali metals. The alkali metal−N_2 distance also lengthens through the series from **2-Na** to **2-Cs** because of the increase in the ionic radius. However, these various changes in the periphery of the complex do not correlate with the extent of back-bonding from iron to N_2, as judged by the N−N distances, the N−N stretching frequency, and the Mössbauer isomer shift.

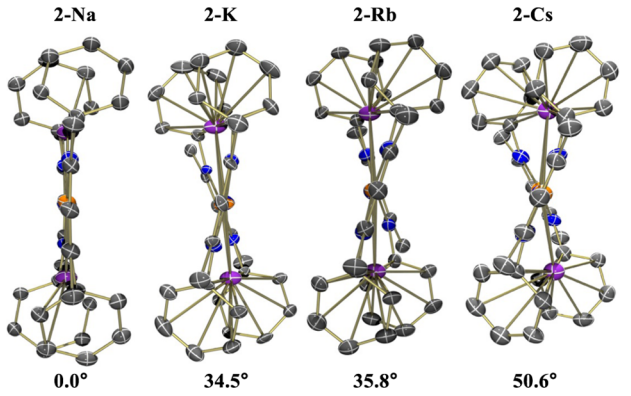

Figure 5. End-on views of **2-AM**, illustrating the twisting of the FeNNFe core as the cation size changes. Torsion angles between the Fe−N−C−C−C−N planes are shown. Isopropyl groups and hydrogens have been omitted for clarity. Thermal ellipsoids are displayed at the 50% probability level.

The crystal structures of **2-K**, **2-Rb**, and **2-Cs** demonstrate the ability of the β-diketiminate-ligand-supported $Fe_2N_2AM_2$ core to accommodate larger cations through rotation of the ligand backbones and aryl groups to create a larger binding pocket for the alkali metal cation. In all three complexes, the alkali cations are centered between the aryl rings of the supporting ligands and also centered above the N_2 unit. Though the N−N distance appears to be longer in **2-Cs**, resonance Raman spectra show only a small decrease in the N−N stretching frequency in going from **2-K** (1625 cm^{-1}) to **2-Cs** (1613 cm^{-1}). These small changes and the indistinguishable isomer shifts of the three complexes suggest that there is very little change in back-bonding from Fe to the dinitrogen and only small changes in N−N bond activation. On the basis of a correlation between the N−N stretching frequency and the N−N distance in transition metal−N_2 complexes,[21a] the expected N−N distance for **2-Cs** is 1.202 Å. Thus, it seems most likely that the crystallographic N−N distance suffers from a systematic error, a conclusion that is consistent with the large thermal ellipsoids for the N atoms that are visible in Figure 3.

We have reported that the diiron(I) complex [$L^{Me}FeNNFeL^{Me}$] readily binds tetrahydrofuran (THF) to form four-coordinate iron species and reacts with benzene to give the iron(I) η^6-benzene complex $L^{Me}Fe(\eta^6\text{-}C_6H_6)$.[13] The iron(0) analogues with the larger cations K^+, Rb^+, and Cs^+ do not bind THF and are stable in C_6D_6 with no change in the ^1H NMR spectrum over the course of 12 h. The reactions of **2-K** and **2-Rb** with 2 equiv of 18-crown-6 result in a mixture of products, none of which is similar spectroscopically to the starting bimetallic species. Identification of these products is ongoing and will be reported separately. Since the alkali metal cations do not appear to influence the electronics or geometry of the Fe−N_2−Fe core and upon extraction of the cations the bimetallic species is no longer present, we attribute the stability of the complexes **2-AM** to the four cation−π interactions between the alkali cations and the arene rings. We have noted similar stabilizing effects of alkali metal cations in highly reduced $Fe_3(\mu\text{-}N_2)_3$ cores and FeSFe cores.[23]

The β-diketiminate supporting ligands can distort through rotation to optimize the size of the binding pocket to comfortably accommodate large cations, which provides stability to the complexes. Intercalation of smaller cations such as Na^+ and Li^+ led to the less stable analogue **2-Na** and in the case of Li^+ gave an unidentifiable mixture of compounds, none of which were spectroscopically similar to the **2-AM** compounds. The presence of two crystallographically independent molecules in the asymmetric unit of **2-Na** offered insight as to why the smaller-cation analogues are less stable. In one molecule, **2-Na (centered)**, the Na^+ ion is centered between the aryl rings with an average Na−C_{aryl} distance of 3.146 Å and the Na−N(N_2) distances differ by less than 0.02 Å. In the other molecule, **2-Na (not centered)**, the Na^+ ion is closer to one of the aryl rings with an average Na−C_{close} distance of 3.017 Å to the close arene ring and an average Na−C_{far} distance of 3.282 Å to the other arene ring. The Na−N(N_2) distances are asymmetric as well, differing by more than 0.1 Å. (It should be noted that in solution **2-Na** exhibits seven ^1H NMR resonances, which is consistent with averaged D_2 symmetry resulting from exchange of the Na^+ between the positions observed in the crystal structure that is fast on the NMR time scale.)

DOI: 10.1021/acs.inorgchem.5b02841
Inorg. Chem. 2016, 55, 2960−2968

Table 2. Fe−Fe Distances, Distances from the Alkali Cations to N_2 and the Aryl Rings, and Torsion Angles between the β-Diketiminate Planes

complex	Fe−Fe (Å)	N−N (Å)	AM−N (Å)	alkali ion−arene centroid (Å)	centroid−centroid (Å)	torsion angle (deg)[a]	alkali ion radius (Å)[c]
2-Na (not centered)[b]	4.709(1)	1.254(6)	2.566(3)	2.675(2)	4.864(2)	0.0(2)	1.02
			2.454(3)	2.975(2)			
2-Na (centered)[b]	4.702(1)	1.253(6)	2.524(3)	2.824(2)	4.830(2)	0.0(2)	1.02
			2.511(3)	2.837(2)			
2-K	4.715(2)	1.215(6)	2.753(6)	2.886(3)	5.229(4)	34.5(3)	1.38
			2.782(6)	2.870(3)	5.400(4)		
			2.792(6)	2.944(3)			
			2.795(6)	2.957(3)			
2-Rb	4.736(2)	1.257(6)	2.918(7)	2.953(3)	5.469(5)	35.8(4)	1.49
			2.931(7)	2.984(3)	5.675(5)		
			2.908(7)	3.041(3)			
			2.869(6)	3.042(3)			
2-Cs[b]	4.751(4)	1.33(2)[d]	3.097(11)	3.141(6)	5.975(8)	50.6(6)	1.67
			3.085(10)	3.160(6)			

[a]The torsion angle was determined by measuring the angle between planes formed from the Fe−N−C−C−C−N atoms of each ligand. [b]Half of the molecule is related by crystallographic symmetry to the other half, and therefore, only one set of distances is given. [c]Values obtained from ref 22 for hexacoordinate alkali cations are given. [d]This value is likely influenced by a systematic error (see the text).

In the analogues with larger cations, the alkali metal ions occupy a single position in the crystal structure centered between the aryl rings and over the N_2 unit. To better understand why the Na^+ compound was not similar to the other three **2-AM** complexes, we compared **2-Na** with other reported complexes with similar η^6 interactions of two arenes with a Na^+ ion. A search of the Cambridge Structural Database (CSD)[24] of reported structures containing such Na^+ species revealed an average Na−C_{aryl} distance of 3.060 Å to the aryl rings. By comparison to the two molecules of **2-Na**, the noncentered molecule has a distance 0.04 Å shorter than the average literature value, while the centered molecule has an average distance 0.1 Å longer than the average literature value. The presence of an off-center molecule in the crystal structure and the unusually long cation−π interaction are consistent with the idea that the Na^+ cations are too small to fit ideally between the aryl rings. This also explains the relatively low stability of **2-Na**.

We were unable to isolate a Li^+ analogue of **2-AM**, which is also consistent with the idea that smaller cations are unable to interact strongly with both aryl rings profitably. By the same approach as for Na^+, a CSD search for η^6-arene−(μ-Li^+)−η^6-arene interactions revealed the average Li−C distance to be 2.497 Å in the reported structures. This value is 0.5 Å shorter than the interactions observed in **2-Na**. We hypothesize that Li^+ is too small to hold the aryl rings together, and without bridging cation−π interactions, the species is unstable (or at least difficult to isolate).

To further understand the stabilizing effect of the cations and discern the relative energies of the complexes, we tested the ability to exchange the alkali cations. This was done by adding triflate salts of other alkali metal ions to solutions of **2-K**, **2-Rb**, and **2-Cs** in THF and monitoring the mixtures by ^{1}H NMR spectroscopy. Each reaction yielded a mixture containing the two previously characterized bimetallic complexes as well as a new product with lower symmetry, as indicated by the number of peaks in the ^{1}H NMR spectrum. Each lower-symmetry product exhibited 13 resonances and chemical shifts between those for the two single-cation complexes, indicating the formation of mixed alkali cation species (which we label **2-MM′**). Thus, **2-K**, **2-Rb**, and **2-Cs** appear to be comparable in stability. Attempts to exchange the cations in **2-Na** were unsuccessful because of the low stability of **2-Na** in THF, so its ability to exchange is unknown.

Computational Analysis of the Dihedral Angle between Fe Planes. One of the surprising aspects of the complexes **2-AM** is that the extent of π back-bonding is similar in all of the complexes despite substantial changes in the dihedral angle between the two diketiminate planes (from 0 to 50.6°). One might have guessed that back-bonding would be maximized when the two ligand planes are perpendicular, because this relative orientation would place the highest-lying half-occupied d orbital (the one in the plane of the diketiminate N donors)[25] of each Fe atom in a position where it does not need to compete for the same π^* orbital of N_2. On the basis of this reasoning, the orientation with coplanar diketiminates should give back-bonding primarily into only one of the two π^* orbitals, leading to less N−N bond activation. However, no correlation between core twisting and back-bonding is evident.

This surprising situation also holds for the previously reported formally diiron(I) complexes LFeNNFeL (L = L^{Me}, L^{tBu}). Three X-ray crystal structures of LFeNNFeL complexes have been reported (Figure 6): one in which the L^{tBu} ligands are perpendicular,[12c] one in which the L^{Me} ligands are coplanar,[13] and yet another where the L^{Me} ligands are coplanar but the iron atom is distorted from a Y shape to a T shape[29] (the latter two structures are for the same compound, but the crystals were grown at different temperatures and yielded different unit cells and different solvents of crystallization). Despite these marked structural differences, there is no sign that the geometry causes substantial differences in N−N back-bonding (Table 3). Though the N−N stretching frequency is lower in the L^{tBu} compound, this is primarily due to an electronic effect, as shown by comparing the difference in the stretching frequencies of [L^{tBu}FeNNFeL^{tBu}] and [L^{Me}FeNNFeL^{Me}] having different orientations ($\Delta\nu$ = 32 cm^{-1}) with the difference in the stretching frequencies of K_2[L^{tBu}FeNNFeL^{tBu}] and K_2[L^{Me}FeNNFeL^{Me}] with the same orientation ($\Delta\nu$ = 36 cm^{-1}).

DOI: 10.1021/acs.inorgchem.5b02841
Inorg. Chem. 2016, 55, 2960−2968

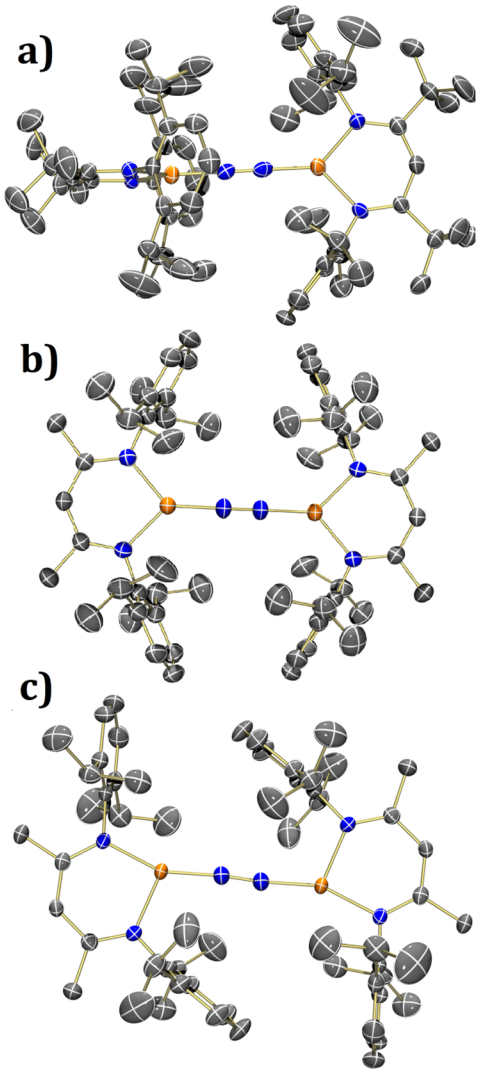

Figure 6. (a) Crystal structure of [$L^{tBu}FeNNFeL^{tBu}$].[12c] (b) Y-shaped crystal structure of [$L^{Me}FeNNFeL^{Me}$].[13] Pentane of crystallization is not shown. (c) T-shaped crystal structure of [$L^{Me}FeNNFeL^{Me}$].[29] In each structure, the thermal ellipsoids are displayed at the 50% probability level. Hydrogen atoms have been omitted for clarity.

Table 3. N−N Bond Distances and Stretching Frequencies for Different Geometries of β-Diketiminate Iron(I) Dinitrogen Complexes

complex	dihedral angle (deg)	N−N (Å)	ν_{NN} (cm^{-1})	ref
[$L^{tBu}FeNNFeL^{tBu}$]	87.2(3)	1.192(6)	1778	12
[$L^{Me}FeNNFeL^{Me}$], Y-shaped	15.7(2)	1.186(7)	1810	29
[$L^{Me}FeNNFeL^{Me}$], T-shaped	9.0(2)	1.172(5)		

DFT calculations were utilized to explore the influence of core distortions on the orbitals and energetics in the FeNNFe core of simple models (details about the calculations are provided in the Supporting Information). Efforts to systematically model the alkali-metal-containing, formally diiron(0) complexes with a range of functionals and basis sets were unsuccessful because geometry optimizations of **2-Na** and **2-Cs** gave diketiminate−diketiminate dihedral angles that did not agree with the experimentally observed structures. Whether these deviations are the result of crystal packing influences or difficulty in computationally reproducing the interaction between the alkali metal ions and the π systems is uncertain, but they prevented us from computationally querying the influence of the alkali metal ion on the diiron(0) core through validated computations.

On the other hand, geometry optimization of the neutral compound $L^{Me,Me}FeNNFeL^{Me,Me}$ (where $L^{Me,Me}$ is a model of L^{Me} in which the isopropyl groups are truncated to methyl groups) at the BP86/TZVP(Fe,N,C)/SVP(H) level gave excellent metrical agreement with the core of the crystallographic structure of $L^{tBu}FeNNFeL^{tBu}$ (Figure 7). In addition,

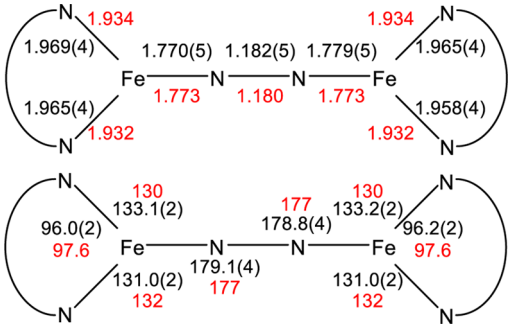

Figure 7. Comparisons of the crystal structure of [$L^{tBu}FeNNFeL^{tBu}$] (black) to the BP86/TZVP(Fe,N,C)/SVP(H) geometry-optimized structure of [$L^{Me,Me}FeNNFeL^{Me,Me}$] (red): (top) comparison of bond lengths (Å); (bottom) comparison of bond angles (deg).

single-point calculations on the optimized septet geometry (using the calibrated TPSSh functional)[26] predicted Mössbauer parameters of δ = 0.56 mm/s and $|\Delta E_Q|$ = 1.27 mm/s, in excellent agreement with the experimentally observed values of δ = 0.62 mm/s and $|\Delta E_Q|$ = 1.41 mm/s. Therefore, more in-depth computational studies on the dependence of the electronic structure on the dihedral angle were pursued through systematic variation of diiron(I) models.

The frontier molecular orbital (MO) energies of LFeNNFeL are illustrated in Figure 8. Mössbauer and solution magnetic studies have shown this molecule to have a septet (S = 3) ground state,[29] and this is the computed spin state that gave excellent metrical and Mössbauer agreement. This suggests that there are six unpaired electrons in nonbonding d orbitals, which come in pairs that have roughly the same energy and differ only in the relationship between the orbitals on the two metal ions. (Plots showing one orbital of each pair are presented in Figure 8.) The frontier orbitals with N_2 character also arise in a pair that differs by rotation by 90° around the Fe−Fe axis. However, in this pair, the α and β electrons have an overlap of only 89%, which is characteristic of "spin polarization".[27] (We note that a broken-symmetry (8,2) calculation gave the same ground state. More details on the computations are given in the Supporting Information.) The α orbitals are more localized on the Fe and the β orbitals are more localized on the N_2, as visualized in the "correlated pair" orbitals in Figure 9.[28] This is suggestive of an electronic structure that is intermediate between the diiron(I)−N_2 resonance structure at the top of Figure 10 and the diiron(II)−N_2^{2-} resonance structure at the bottom of Figure 10 (the latter has two high-spin iron(II) ions and a triplet dinitrogen, with strong antiferromagnetic coupling between the N_2^{2-} and each of the Fe ions). This electronic structure model

DOI: 10.1021/acs.inorgchem.5b02841
Inorg. Chem. 2016, 55, 2960−2968

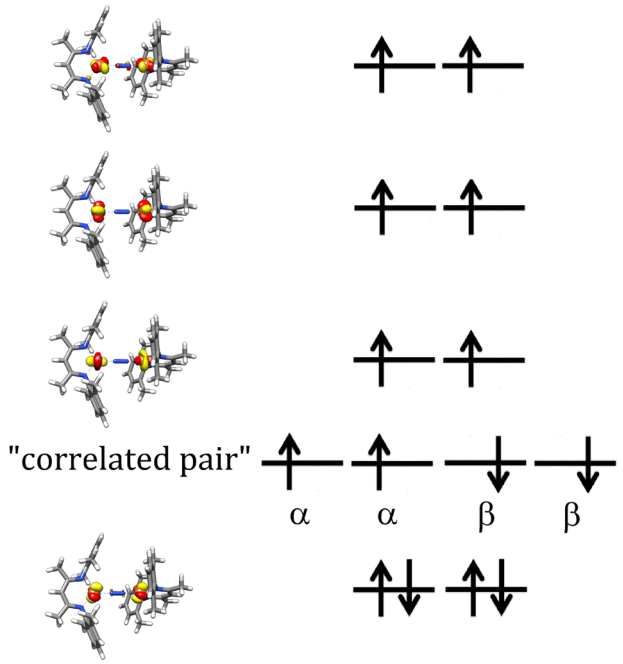

Figure 8. Electronic structure of [$L^{Me,Me}$FeNNFe$L^{Me,Me}$] computed at the BP86/TZVP(Fe,N,C)/SVP(H) level in the experimentally demonstrated septet (S = 3) ground state. "Correlated pair" α and β orbitals are shown in Figure 9.

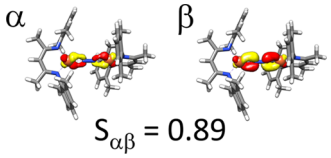

Figure 9. "Correlated pair" from Figure 8, showing an α orbital localized on Fe and a β orbital localized on the N_2 unit with an overlap of 0.89. The other pair of correlated α and β orbitals have the same appearance but are rotated 90° from these.

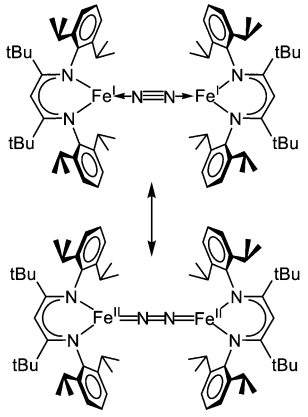

Figure 10. Resonance structures of [L^{tBu}FeNNFeL^{tBu}]. (top) diiron(I) with ferromagnetic coupling and a neutral N_2 unit, yielding S = 3; (bottom) diiron(II) antiferromagnetically coupled to a triplet N_2^{2-} unit, yielding S = 3.

was previously presented on the basis of variable-field Mössbauer studies of L^{Me}FeNNFeL^{Me}.[29]

In order to explore the interplay of the electronic and geometric structures, we constrained the model of $L^{Me,Me}$FeNNFe$L^{Me,Me}$ to have a dihedral angle of 0° between the two FeN_3 planes. Interestingly, the BP86-optimized model had very similar N–N distances (Δ_{N-N} = 0.002 Å) and Fe–N distances (Δ_{Fe-N} = 0.006 Å) that are close enough to be experimentally indistinguishable. The predicted Mössbauer parameters for the coplanar structure are δ = 0.54 mm/s and $|\Delta E_Q|$ = 1.54 mm/s, which are also within the expected uncertainty limits of the experimentally observed values. In addition, the energy of the optimized structure was nearly the same after planarization of the core (+4 kcal/mol using BP86; 0 kcal/mol using TPSSh). These results suggest that twisting around the FeNNFe axis has little energetic influence on the core, consistent with the observation that both parallel and perpendicular structures have been observed for the LFeNNFeL cores. In addition, the geometry optimization of the coplanar model gave a substantial lateral twist at each Fe atom to give asymmetric N(diketiminate)–Fe–N(N_2) angles of 115° and 148°, which are close to the angles of 110° and 155° observed in the T-shaped crystal form of L^{Me}FeNNFeL^{Me} (Figure 6c). Thus, the change from a Y shape to a T shape at iron is also inconsequential with respect to the energy of the molecule.

In order to explore the influence of rotation in more detail, the dihedral angle between the two FeN_3 planes was varied between 0° and 90° in 10° steps using a simplified model where the diketiminates were further truncated to $N_2C_3H_5$ (L^{trunc}). The BP86-calculated energies vary smoothly over a range of only 2 kcal/mol (Figure 11). Why are these changes so small?

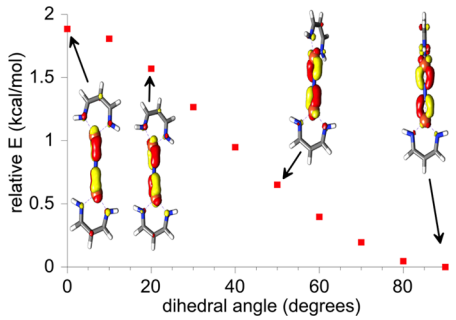

Figure 11. Computed relative energies of [L^{trunc}FeNNFeL^{trunc}] as the dihedral angle between the diketiminate ligands is varied from 0° to 90°. It should be noted that the change in energy is less than 2 kcal/mol. The insets show one of the two perpendicular Fe–N_2 back-bonding orbitals (MO 63) at different dihedral angles.

Examination of the key N_2 back-bonding orbitals (MOs 63 and 64; Figure 12, bottom left) shows that they are degenerate in the D_{2d} structure with its 90° dihedral angle (same energy at the bottom right in Figure 12) because they lie in the mirror planes that contain the perpendicular C_2 (or C_2') axes. As the molecule twists through intermediate geometries (having D_2 symmetry) toward the geometry having D_{2h} symmetry with its dihedral angle of 0°, the back-bonding orbitals rotate to follow the C_2 axes that are perpendicular to the FeNNFe vector rather than the ligand planes themselves. Additionally, the energies of MOs 63 and 64 compensate for one another (blue and green lines in Figure 12). This indicates that the interaction between the Fe atomic orbitals and the N_2 π^* orbitals can change but that the gain in energy of one MO is balanced by a loss of energy of the other through the entire range of accessible dihedral angles.

Visualization of the frontier orbitals also shows that one of the orbitals (MO 72; red box in Figure 12), which is a

DOI: 10.1021/acs.inorgchem.5b02841
Inorg. Chem. 2016, 55, 2960–2968

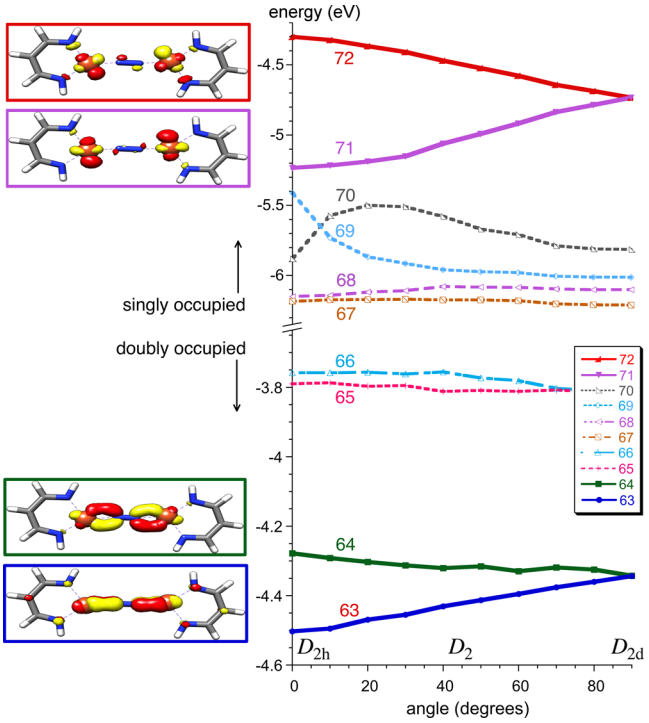

Figure 12. Walsh diagrams of high-lying molecular orbitals of $L^{trunc}FeNNFeL^{trunc}$, showing the changes in the energies of the MOs through a scan of the dihedral angle between the ligands from 0° to 90°. The top part shows singly occupied orbitals (α only), and the bottom part shows doubly occupied orbitals. Example orbitals (with dihedral angle = 0°) are pictured on the left side, with the box colors corresponding to the line colors in the Walsh diagrams.

nonbonding d orbital in the 90° structure, gains Fe−N_2 antibonding character upon twisting of the Fe from a Y shape to a T shape, and its energy increases. However, lowering of the energy of its partner, MO 71, compensates for this.

Overall, these computational results show that the surprisingly small influence of distortion on the energy comes from flexible interactions of Fe with N_2, where the in-plane and out-of-plane orbitals can mix in such a way to maintain similar back-bonding. Computations on an optimized, all-atom model of $K_2[L^{Me}FeNNFeL^{Me}]$ suggest that the frontier orbitals are similar to those in LFeNNFeL as described above, except that the positive charge of the potassium ions causes a lowering of the energy of the key N_2 π^* orbitals. The aforementioned difficulties in reproducing the experimental geometries prevented us from systematically examining the influence of the dihedral angle on the formally diiron(0) complexes, but it is reasonable to hypothesize that similar compensatory factors are at play.

CONCLUSION AND PERSPECTIVES

We have demonstrated the ability of β-diketiminate ligands to accommodate varying sizes of alkali metal cations (Na^+, K^+, Rb^+, Cs^+), and we have shown that these cations exert their primary influence on the stability of the complexes by holding the aryl rings of the supporting ligands together. Ultimately, the charge of the cation has the greatest influence on the connectivity of the complexes: it should be noted that the dicationic alkaline earth cation Mg^{2+} gives M−N_2−Mg−N_2−M cores that are distinct from those described here.[30] Within the alkali metals, the only major change is a rotation around the FeNNFe axis. Computational models support the idea that the rotation does not modify the extent of N−N bond activation and explain the surprising lack of geometric preferences through mixing of key d orbitals that gives similar back-bonding into the π^* orbitals of N_2 irrespective of the relative orientation of the supporting ligands.

In previous work with a smaller diketiminate ligand, we observed that the choice of alkali metal can influence the shape of trimetallic and tetrametallic iron−N_2 clusters and concluded that the influence was primarily from the size of the cation and its ability to fit in the appropriate space between the aromatic rings and N_2.[23a] The current work indicates a similar conclusion for bimetallic complexes: the main differences arise from size matching between the cation and the available space near the Fe−N_2 core and the aryl groups. It is thus reasonable to speculate that there will be other opportunities to vary the size of the alkali metals to tune the geometry of other low-valent complexes.

ASSOCIATED CONTENT

Supporting Information

The Supporting Information is available free of charge on the ACS Publications website at DOI: 10.1021/acs.inorgchem.5b02841.

Crystallographic details (CIF)
Synthetic, spectroscopic, crystallographic, and computational data (PDF)

AUTHOR INFORMATION

Corresponding Author

*E-mail: patrick.holland@yale.edu.

Present Address

§K.G.: Pacific Northwest National Laboratory, 902 Battelle Boulevard, Richland, WA 99352.

Notes

The authors declare no competing financial interest.

ACKNOWLEDGMENTS

This work was supported by the National Institutes of Health (GM065313 to P.L.H.; GM116463 to S.F.M.). We thank Frank Neese and Shengfa Ye (Max Planck Institute for Chemical Energy Conversion, Mülheim an der Ruhr, Germany) for assistance and resources for some of the computations, which were performed during sabbatical work by P.L.H. and funded by the Germany Fulbright Commission.

REFERENCES

(1) (a) Hidai, M.; Mizobe, Y. *Chem. Rev.* **1995**, *95*, 1115−1133. (b) Fryzuk, M. D.; Johnson, S. A. *Coord. Chem. Rev.* **2000**, *200*−*202*, 379−409. (c) Gambarotta, S.; Scott, J. *Angew. Chem., Int. Ed.* **2004**, *43*, 5298−5308. (d) MacKay, B. A.; Fryzuk, M. D. *Chem. Rev.* **2004**, *104*, 385−402.

(2) Nielsen, A. *Ammonia: Catalysis and Manufacture*; Springer: Berlin, 1995.

(3) Schlögl, R. In *Handbook of Heterogeneous Catalysis*, 2nd ed.; Wiley-VCH: Weinheim, Germany, 2008; Vol. *5*, p 2501−2575.

(4) (a) Burgess, B. K. *Chem. Rev.* **1990**, *90*, 1377−1406. (b) Burgess, B. K.; Lowe, D. J. *Chem. Rev.* **1996**, *96*, 2983−3012.

(5) (a) Hoffman, B. M.; Dean, D. R.; Seefeldt, L. C. *Acc. Chem. Res.* **2009**, *42*, 609−619. (b) Ertl, G. *J. Vac. Sci. Technol., A* **1983**, *1*, 1247−1253.

(6) (a) Dumesic, J. A.; Topsøe, H.; Boudart, M. *J. Catal.* **1975**, *37*, 513−522. (b) Spencer, N. D.; Schoonmaker, R. C.; Somorjai, G. A. *J.*

DOI: 10.1021/acs.inorgchem.5b02841
Inorg. Chem. 2016, 55, 2960−2968

Catal. **1982**, *74*, 129−135. (c) Falicov, L. M.; Somorjai, G. A. *Proc. Natl. Acad. Sci. U. S. A.* **1985**, *82*, 2207−2211. (d) Strongin, D. R.; Carrazza, J.; Bare, S. R.; Somorjai, G. A. *J. Catal.* **1987**, *103*, 213−215. (e) Mortensen, J. J.; Hansen, L. B.; Hammer, B.; Nørskov, J. K. *J. Catal.* **1999**, *182*, 479−488.
(7) Ertl, G.; Weiss, M.; Lee, S. B. *Chem. Phys. Lett.* **1979**, *60*, 391−394.
(8) Ertl, G.; Lee, S. B.; Weiss, M. *Surf. Sci.* **1982**, *114*, 527−545.
(9) Ung, G.; Peters, J. C. *Angew. Chem., Int. Ed.* **2015**, *54*, 532−535.
(10) (a) Hazari, N. *Chem. Soc. Rev.* **2010**, *39*, 4044−4056. (b) Köthe, C.; Limberg, C. *Z. Anorg. Allg. Chem.* **2015**, *641*, 18−30.
(11) (a) Tondreau, A. M.; Stieber, S. C. E.; Milsmann, C.; Lobkovsky, E.; Weyhermüller, T.; Semproni, S. P.; Chirik, P. J. *Inorg. Chem.* **2013**, *52*, 635−646. (b) Peters, J. C.; Cherry, J.-P. F.; Thomas, J. C.; Baraldo, L.; Mindiola, D. J.; Davis, W. M.; Cummins, C. C. *J. Am. Chem. Soc.* **1999**, *121*, 10053−10067. (c) Cherry, J.-P. F.; Stephens, F. H.; Johnson, M. J. A.; Diaconescu, P. L.; Cummins, C. C. *Inorg. Chem.* **2001**, *40*, 6860−6862. (d) Yandulov, D. V.; Schrock, R. R. *Can. J. Chem.* **2005**, *83*, 341−357. (e) Moret, M.-E.; Peters, J. C. *Angew. Chem., Int. Ed.* **2011**, *50*, 2063−2067. (f) Lee, Y.; Mankad, N. P.; Peters, J. C. *Nat. Chem.* **2010**, *2*, 558−565. (g) Creutz, S. E.; Peters, J. C. *J. Am. Chem. Soc.* **2014**, *136*, 1105−1115.
(12) (a) Pfirrmann, S.; Limberg, C.; Herwig, C.; Stößer, R.; Ziemer, B. *Angew. Chem., Int. Ed.* **2009**, *48*, 3357−3361. (b) Ding, K.; Pierpont, A. W.; Brennessel, W. W.; Lukat-Rodgers, G.; Rodgers, K. R.; Cundari, T. R.; Bill, E.; Holland, P. L. *J. Am. Chem. Soc.* **2009**, *131*, 9471−9472. (c) Smith, J. M.; Lachicotte, R. J.; Pittard, K. A.; Cundari, T. R.; Lukat-Rodgers, G.; Rodgers, K. R.; Holland, P. L. *J. Am. Chem. Soc.* **2001**, *123*, 9222−9223. (d) Horn, B.; Pfirrmann, S.; Limberg, C.; Herwig, C.; Braun, B.; Mebs, S.; Metzinger, R. *Z. Anorg. Allg. Chem.* **2011**, *637*, 1169−1174.
(13) Smith, J. M.; Sadique, A. R.; Cundari, T. R.; Rodgers, K. R.; Lukat-Rodgers, G.; Lachicotte, R. J.; Flaschenriem, C. J.; Vela, J.; Holland, P. L. *J. Am. Chem. Soc.* **2006**, *128*, 756−769.
(14) (a) Bonomo, L.; Stern, C.; Solari, E.; Scopelliti, R.; Floriani, C. *Angew. Chem., Int. Ed.* **2001**, *40*, 1449−1452. (b) Ferguson, R.; Solari, E.; Floriani, C.; Chiesi-Villa, A.; Rizzoli, C. *Angew. Chem., Int. Ed. Engl.* **1993**, *32*, 396−397. (c) Caselli, A.; Solari, E.; Scopelliti, R.; Floriani, C.; Re, N.; Rizzoli, C.; Chiesi-Villa, A. *J. Am. Chem. Soc.* **2000**, *122*, 3652−3670. (d) Evans, W. J.; Fang, M.; Zucchi, G.; Furche, F.; Ziller, J. W.; Hoekstra, R. M.; Zink, J. I. *J. Am. Chem. Soc.* **2009**, *131*, 11195−11202. (e) Fout, A. R.; Basuli, F.; Fan, H.; Tomaszewski, J.; Huffman, J. C.; Baik, M.-H.; Mindiola, D. J. *Angew. Chem., Int. Ed.* **2006**, *45*, 3291−3295. (f) Pun, D.; Bradley, C. A.; Lobkovsky, E.; Keresztes, I.; Chirik, P. J. *J. Am. Chem. Soc.* **2008**, *130*, 14046−14047. (g) Scott, J.; Vidyaratne, I.; Korobkov, I.; Gambarotta, S.; Budzelaar, P. H. M. *Inorg. Chem.* **2008**, *47*, 896−911. (h) Semproni, S. P.; Knobloch, D. J.; Milsmann, C.; Chirik, P. J. *Angew. Chem., Int. Ed.* **2013**, *52*, 5372−5376. (i) Weare, W. W.; Schrock, R. R.; Hock, A. S.; Müller, P. *Inorg. Chem.* **2006**, *45*, 9185−9196.
(15) (a) Grunze, M.; Golze, M.; Hirschwald, W.; Freund, H. J.; Pulm, H.; Seip, U.; Tsai, M. C.; Ertl, G.; Küppers, J. *Phys. Rev. Lett.* **1984**, *53*, 850−853. (b) Freund, H. J.; Bartos, B.; Messmer, R. P.; Grunze, H.; Kuhlenbeck, H.; Neumann, M. *Surf. Sci.* **1987**, *185*, 187−202.
(16) Chen, C.; Bellows, S. M.; Holland, P. L. *Dalton Trans.* **2015**, *44*, 16654−70.
(17) For the nickel system, a mixed-valent $Ni^{I}Ni^{0}$ species containing only one potassium has been isolated; it has N−N bond metrics between those of the Ni^{I}_{2} and Ni^{0}_{2} complexes, as expected. See ref 12a.
(18) Klissurski, D. G.; Mitov, I. G.; Tomov, T. *Stud. Surf. Sci. Catal.* **1983**, *16*, 421−430.
(19) (a) Tonzetich, Z. J.; Héroguel, F.; Do, L. H.; Lippard, S. J. *Inorg. Chem.* **2011**, *50*, 1570−1579. (b) Dugan, T. R. Ph.D. Dissertation, University of Rochester, Rochester, NY, 2012.
(20) Huber, K. P.; Herzberg, G. *Molecular Spectra and Molecular Structure. IV. Constants of Diatomic Molecules*; Van Nostrand Reinhold: New York, 1979.
(21) (a) Holland, P. L. *Dalton Trans.* **2010**, *39*, 5415−5425. (b) Shimanouchi, T. Molecular Vibrational Frequencies. In *NIST Chemistry WebBook*; Linstrom, P. J., Mallard, W. G., Eds.; NIST Standard Reference Database Number 69; National Institute of Standards and Technology: Gaithersburg, MD; http://webbook.nist.gov (accessed Aug 26, 2015).
(22) Shannon, R. D. *Acta Crystallogr., Sect. A: Cryst. Phys., Diffr., Theor. Gen. Crystallogr.* **1976**, *32*, 751−767.
(23) (a) Grubel, K.; Brennessel, W. W.; Mercado, B. Q.; Holland, P. L. *J. Am. Chem. Soc.* **2014**, *136*, 16807−16816. (b) Rodriguez, M. M.; Stubbert, B. D.; Scarborough, C. C.; Brennessel, W. W.; Bill, E.; Holland, P. L. *Angew. Chem., Int. Ed.* **2012**, *51*, 8247−8250.
(24) Allen, F. H. *Acta Crystallogr., Sect. B: Struct. Sci.* **2002**, *58*, 380−388.
(25) Holland, P. L.; Cundari, T. R.; Perez, L. L.; Eckert, N. A.; Lachicotte, R. J. *J. Am. Chem. Soc.* **2002**, *124*, 14416−14424.
(26) Römelt, M.; Ye, S.; Neese, F. *Inorg. Chem.* **2009**, *48*, 784−785.
(27) Jacob, C. R.; Reiher, M. *Int. J. Quantum Chem.* **2012**, *112*, 3661.
(28) (a) Neese, F. *J. Phys. Chem. Solids* **2004**, *65*, 781. (b) Dugan, T. R.; Bill, E.; MacLeod, K. C.; Christian, G. J.; Cowley, R. E.; Brennessel, W. W.; Ye, S.; Neese, F.; Holland, P. L. *J. Am. Chem. Soc.* **2012**, *134*, 20352−20364.
(29) Stoian, S. A.; Vela, J.; Smith, J. M.; Sadique, A. R.; Holland, P. L.; Münck, E.; Bominaar, E. L. *J. Am. Chem. Soc.* **2006**, *128*, 10181−10192.
(30) Dugan, T. R.; MacLeod, K. C.; Brennessel, W. W.; Holland, P. L. *Eur. J. Inorg. Chem.* **2013**, *2013*, 3891−3897.

DOI: 10.1021/acs.inorgchem.5b02841
Inorg. Chem. 2016, 55, 2960−2968